National Research Centre **“Kurchatov Institute”**

A.A. Logunov INSTITUTE FOR HIGH ENERGY PHYSICS
of the National Research Centre “Kurchatov Institute”

Polarization of hyperons produced by meson beams

V.V. Abramov, IHEP, Protvino

XIX Workshop on High Energy Spin Physics, DSPIN-23 (Efremov-90)

Dubna, Russia, September 5, 2023

Объединенный институт ядерных исследований
НАУКА СБЛИЖАЕТ НАРОДЫ

Talk content

1. **Introduction**

2. **The Chromo-magnetic polarization of quarks (CPQ) model**

3. **Existing data for $P_N(x_F, p_T)$ in $\pi^{\pm}(K^{\pm})+ p(A) \rightarrow \Lambda(\tilde{\Lambda}) + X$**

4. **The CPQ model predictions for $P_N(x_F, p_T, \sqrt{s}, A)$**

5. **Conclusions and outlook**

Introduction

The polarization of Λ-hyperons and the corresponding antihyperons has a rich phenomenology that has not yet received a convincing explanation. The polarization depends on the type of reaction, kinematic variables, and the atomic weight of the target. The study the of polarization dependence on these variables will make it possible to advance in revealing the mechanism of large polarization effects, observed in dozens of reactions. Meson beams are of particular interest in such studies because they contain valence quarks and antiquarks of various flavors, including strange quarks and antiquarks.

These data are used to determine the parameters of the model of chromomagnetic polarization of quarks(CPQ)[1, 2]. Dependences predicted by the CPQ model can later be tested in experiments at the U-70 accelerator at the National Research Center “Kurchatov Institute” - IHEP (at the SPASCHARM facility).

The CPQ model predicts a number of interesting effects that may be critical for understanding the nature of polarization phenomena.

Model of chromomagnetic polarization of quarks (CPQ)

The CPQ model can be considered as a generalization of empirical laws found in the course of global data analysis, as well as a number of ideas related to the interaction of quarks in the quark confinement region [1,2]. The global analysis includes 96 inclusive and 29 exclusive reactions with a total of 7730 experimental data points, which makes it possible to determine the model global parameters with high accuracy.

A circular transverse chromomagnetic field in the hadron interaction region exists [Migdal,1985]. The interaction of the chromomagnetic moments of quarks with this inhomogeneous chromomagnetic field leads to their polarization (similar to the polarization of electrons in the famous Stern-Gerlach experiment) [Ryskin,1988].

In the CPQ model a circular transverse chromomagnetic field B^a is created by spectator quarks and antiquarks moving in the cm in forward and backward directions. The initial region of interaction of hadrons in the cm shown in Fig. 1 in red. Spectator quarks and active test quarks (which will be part of the observed hyperon) fly out of this region.

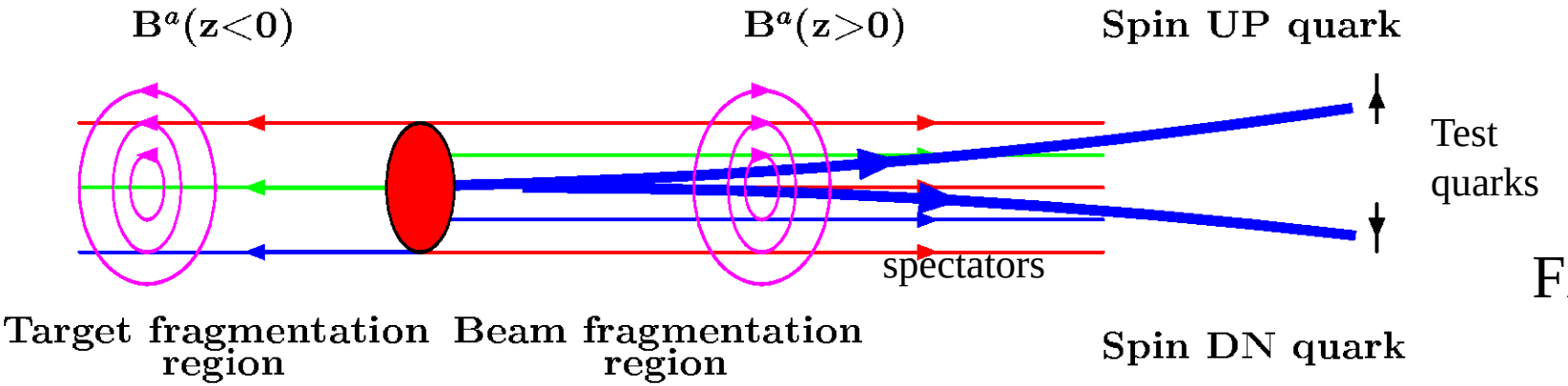

Fig. 1

Model of chromomagnetic polarization of quarks (CPQ)

$\boldsymbol{\mu}^{a}_{Q} = s g^{a} g_{s}/2M_{Q}$ – the chromomagnetic dipole moment of the constituent quark Q interacts with the inhomogeneous chromomagnetic field and Stern-Gerlach force arises. The Stern-Gerlach force acts on the test quark (which will be a part of the detected hadron) and gives it a p_T kick to the left or right, depending on quark polarization.

The field gradient has the same direction to the left and right relative to the collision axis, which provides a non-zero polarization effect.

An active test quark trajectory (shown as a blue curve in Fig.1) deviates predominantly to the left or right in an inhomogeneous field B^a, depending on the direction of its spin relative to the normal to the hyperon production plane.

In addition to the action of the Stern-Gerlach force on a quark in a chromomagnetic field, the precession of the quark spin in this field takes place, which in the case of strong fields leads to oscillations of P_N on x_F and other variables, which is one of the main features of the CPQ model. For a number of reactions, the CPQ model predicts the dependence of P_N on $\sqrt{s}$ of the resonance type due to the dependence of the quark spin precession rate on its energy.

The polarization data were transformed according to a single convention, in which for a hyperon scattered to the left and having a downward spin, the polarization is considered negative.

2 Data on the polarization of Λ-hyperons in K^- meson beam

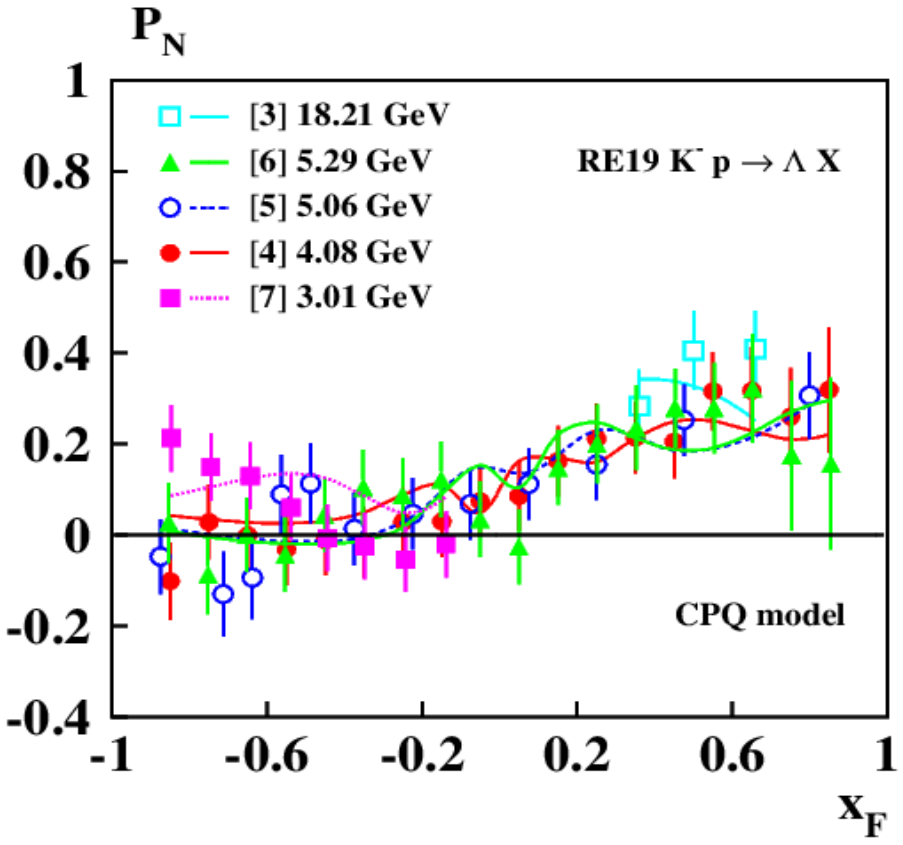

Fig. 2. Data and calculations using the CPQ $P_N(x_F)$ model for the reaction $K^- + p \rightarrow \Lambda + X$.

Data on $P_N(x_F)$ for the reaction $K^- + p \rightarrow \Lambda + X$ in the energy range $3.01 \leq \sqrt{s} \leq 18.21$ GeV [3-7] are shown in Fig. 2. In the same place, colored lines show the calculated values of polarization according to the CPQ model. The energy value $\sqrt{s}$ is shown in Fig. 2 and following next to the publication reference number. The data indicate that the polarization depends on $\sqrt{s}$ and x_F. The maximum positive polarization is observed in the region $x_F > 0.2$. In this reaction, the valence strange s-quark from the K^- meson is an active test quark that passes into the observed Λ-hyperon.

Polarization of Λ-antihyperons in the reaction $K^+ + p \rightarrow \tilde{\Lambda} + X$

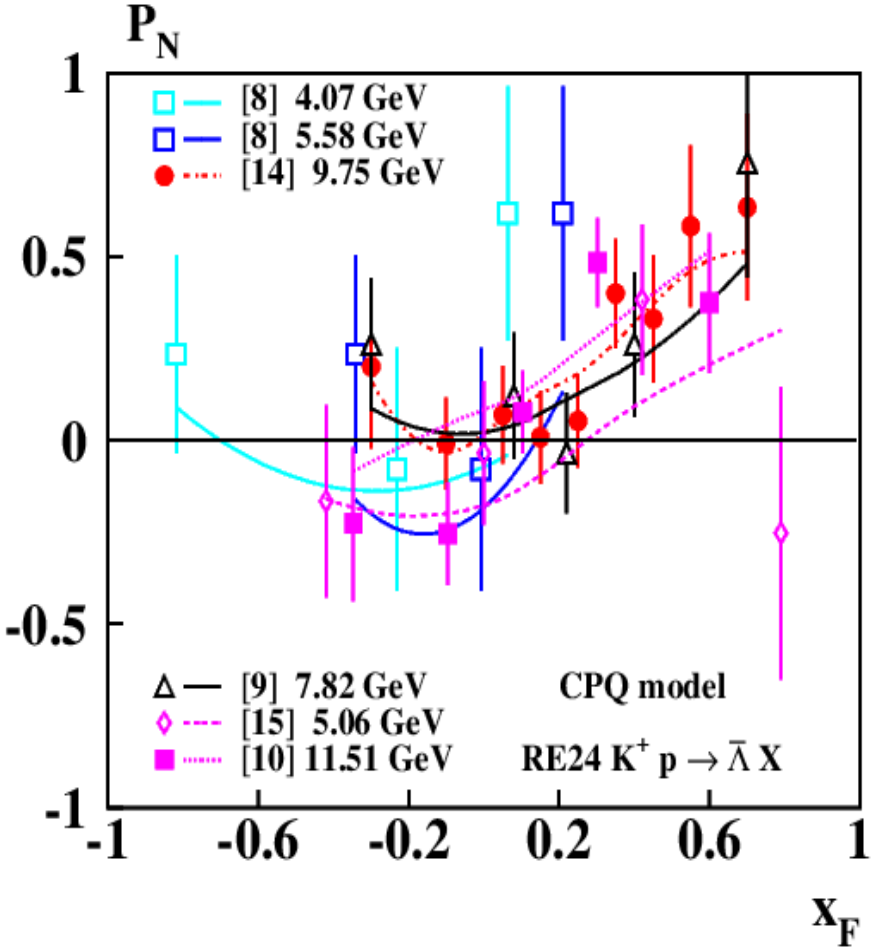

Fig. 3. Data and calculations using the CPQ $P_N(x_F)$ model for the reaction $K^+ + p \rightarrow \tilde{\Lambda} + X$.

The data on the dependence $P_N(x_F)$ for the reaction $K^+ + p \rightarrow \tilde{\Lambda} + X$ in the energy range $3.86 \leq \sqrt{s} \leq 11.51$ GeV [5,6,7] are shown in Fig. 73 There is agreement between the calculations and data, and an increase in $P_N(x_F)$ is predicted in the range of positive values of the Feynman variable x_F.

Comparison of Fig. 2 and Fig. 3 shows some similarity in the behavior of $P_N(x_F)$ for these two reactions when replacing a particle with an antiparticle for the beam and the observed hyperon. In both cases we have the heavy valence strange quark (antiquark) passing into the observed hyperon (antihyperon).

Polarization of Λ-hyperons in the reaction $K^+ + p \rightarrow \Lambda + X$

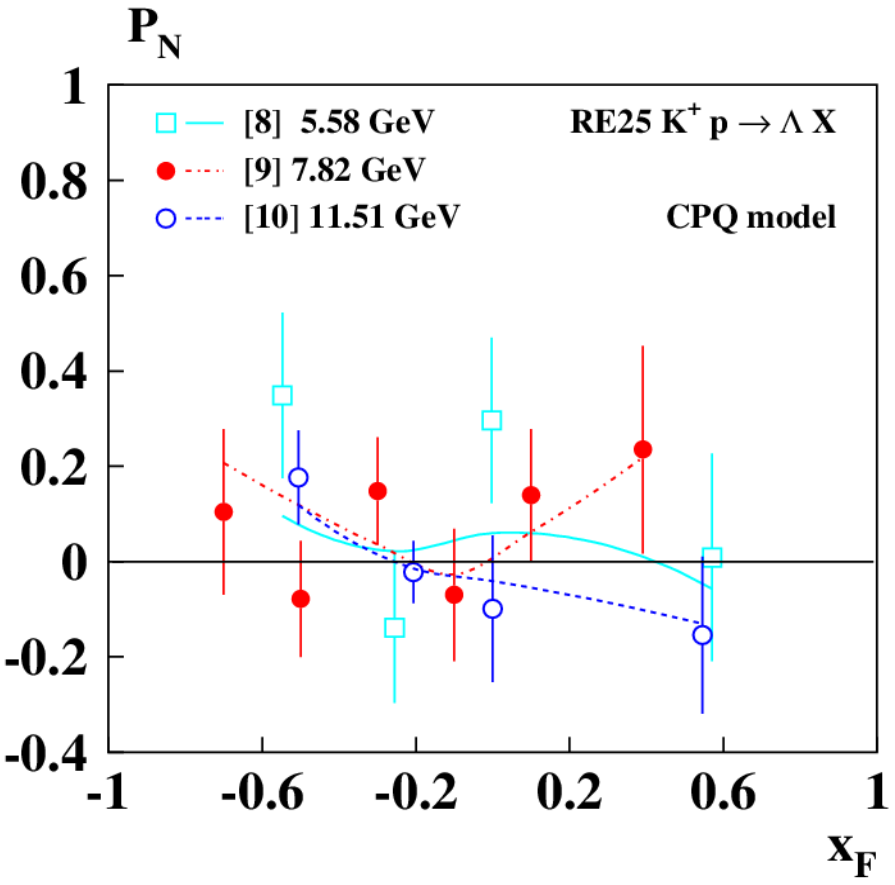

Fig. 4. Data and calculations using the CPQ $P_N(x_F)$ model for the reaction $K^+ + p \rightarrow \Lambda + X$.

Data on the dependence $P_N(x_F)$ for the reaction $K^+ + p \rightarrow \Lambda + X$ in the energy range $5.58 \leq \sqrt{s} \leq 11.51$ GeV [8-10] are shown in Fig. 4. The data indicate some dependence of the polarization on $\sqrt{s}$ and x_F, which is reproduced within the CPQ model. However, the accuracy of the data does not allow us to draw definite conclusions about the dependence on kinematic variables.

It can be noted that the active valence quark from the beam, passing into the observed Λ-hyperon, here is the light u-quark, not s-quark.

Polarization of Λ-antihyperons in K^- meson beam

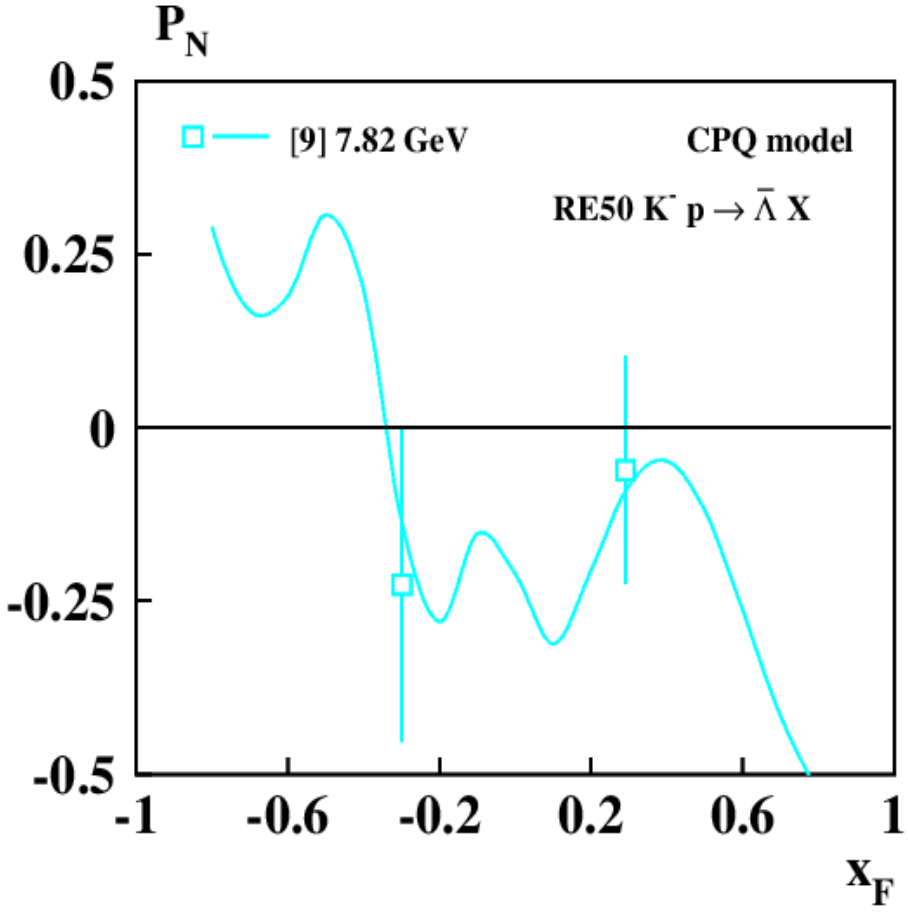

Fig. 5. Data and calculations using the CPQ $P_N(x_F)$ model for the reaction $K^- + p \to \tilde{\Lambda} + X$.

The data on the $P_N(x_F)$ dependence for the reaction $K^- + p \to \tilde{\Lambda} + X$ at the energy $\sqrt{s}$=7.82 GeV [9] are shown in Fig. 5. A feature of the dependence $P_N(x_F)$ for this reaction is its oscillation, which is predicted within the framework of the CPQ model. The accuracy and amount of available data, as in most other reactions considered in the work, is insufficient to determine the dependences on kinematic variables.

To resolve the ambiguity of the polarization behaviour, additional data are required in various kinematic regions.

Polarization of Λ-hyperons in the reaction $\pi^- + p \rightarrow \Lambda + X$

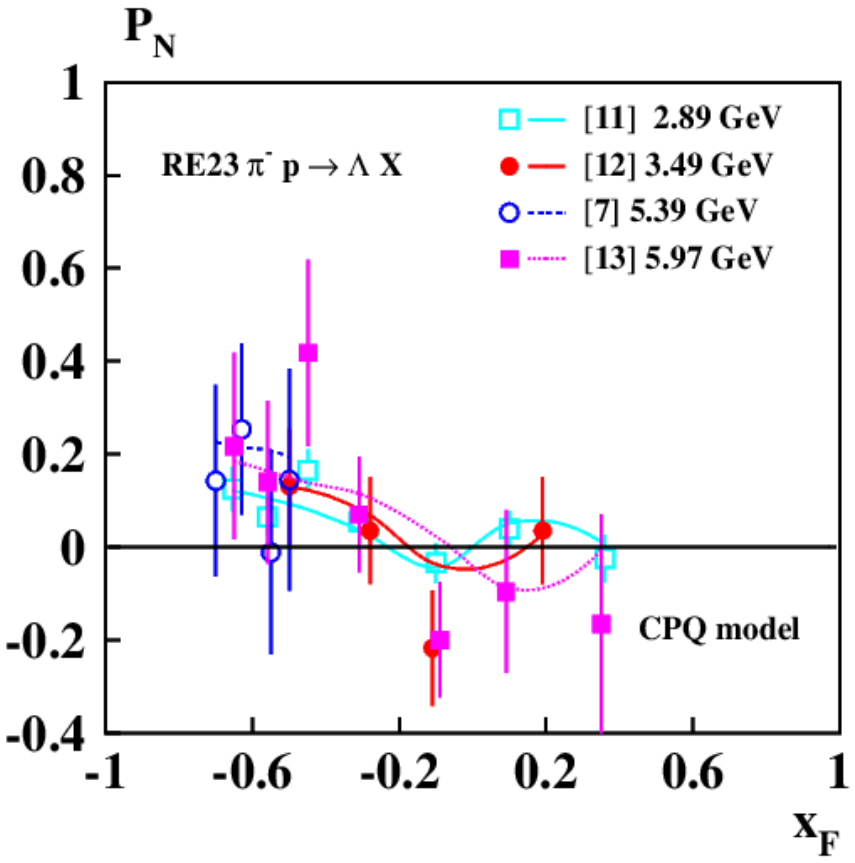

Fig. 6. Data and calculations using the CPQ $P_N(x_F)$ model for the reaction $\pi^- + p \rightarrow \Lambda + X$.

Data on the dependence $P_N(x_F)$ for the reaction $\pi^- + p \rightarrow \Lambda + X$ in the energy range $2.89 \leq \sqrt{s} \leq 5.97$ GeV [11,12,7,13] are shown in Fig. 6. Significant positive polarization is observed in the region of target fragmentation, at x_F of the order of -0.6. The CPQ model describes the observed behavior of the data.

Comparison of data in Fig. 2 and 6 indicates that replacing the K^- beam with π^- leads to almost zero polarization in the $x_F>0$ region, and $P_N(x_F) >0$ for $x_F<0$.

The active valence d-quark from the π^-, passing into the Λ-hyperon, does not lead to its polarization, since the spin of the Λ-hyperon in the naive quark model is carried over by the s-quark .

Polarization of Λ-hyperons in the reaction $\pi^+ + p \rightarrow \Lambda + X$

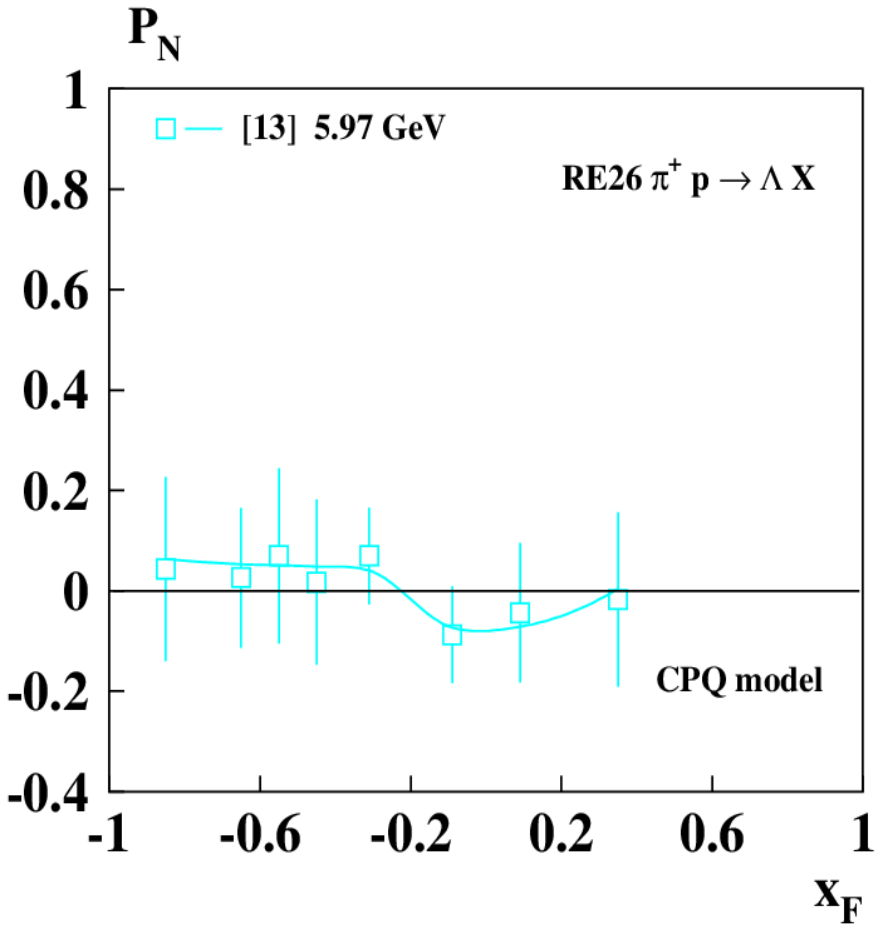

Fig. 7. Data and calculations using the CPQ $P_N(x_F)$ model for the reaction $\pi^+ + p \rightarrow \Lambda + X$.

The data on the dependence $P_N(x_F)$ for the reaction $\pi^+ + p \rightarrow \Lambda + X$ at an energy of $\sqrt{s}$=5.97 GeV [13] are shown in Fig. 7, where they are compared with calculations based on the CPQ model. The polarization $P_N(x_F)$ at the energy indicated above is negligible, compatible with zero.

For positive x_F region the polarization in reactions $\pi^- + p \rightarrow \Lambda + X$ and $\pi^+ + p \rightarrow \Lambda + X$ looks similar.

Polarization of Λ-antihyperons in the reaction $\pi^- + p \rightarrow \tilde{\Lambda} + X$

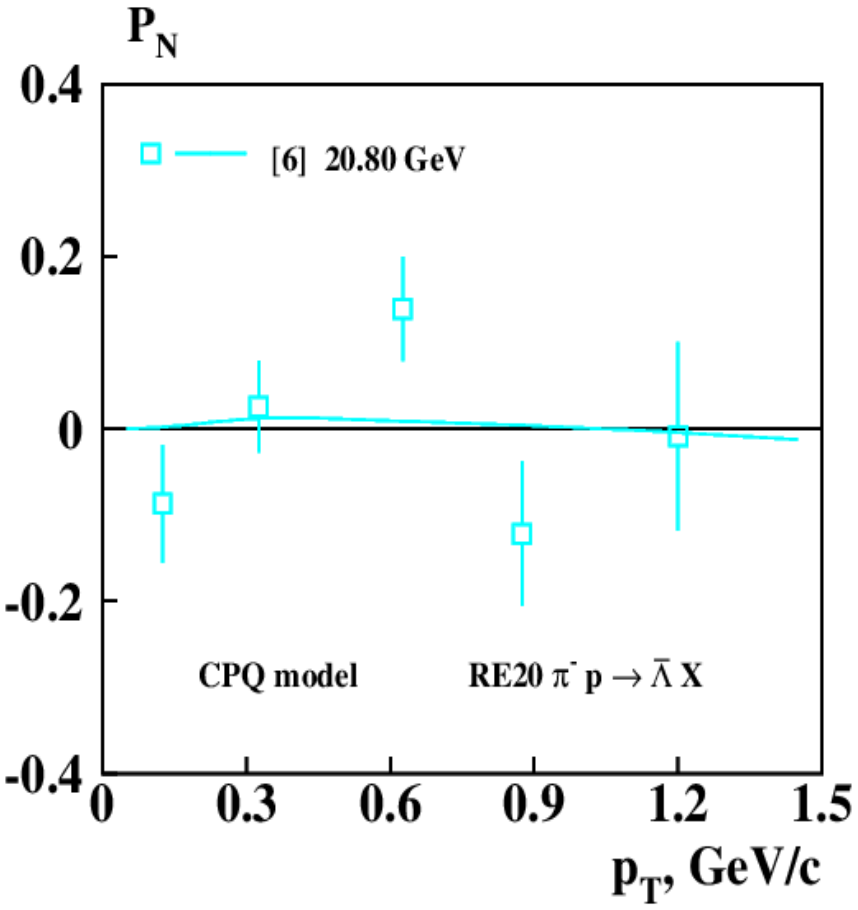

Fig. 8. Data and calculations using the CPQ $P_N(p_T)$ model for the reaction $\pi^- + p \rightarrow \tilde{\Lambda} + X$.

The data on the dependence $P_N(p_T)$ for the reaction $\pi^- + p \rightarrow \tilde{\Lambda} + X$ at the energy $\sqrt{s}$=20.8 GeV [6] are shown in Fig. 8, where they are compared with the calculations based on the CPQ model.

The CPQ model predicts a negligible value for $P_N(p_T)$ in this particular kinematic region.

Calculations of the polarization of Λ-hyperons in meson beams

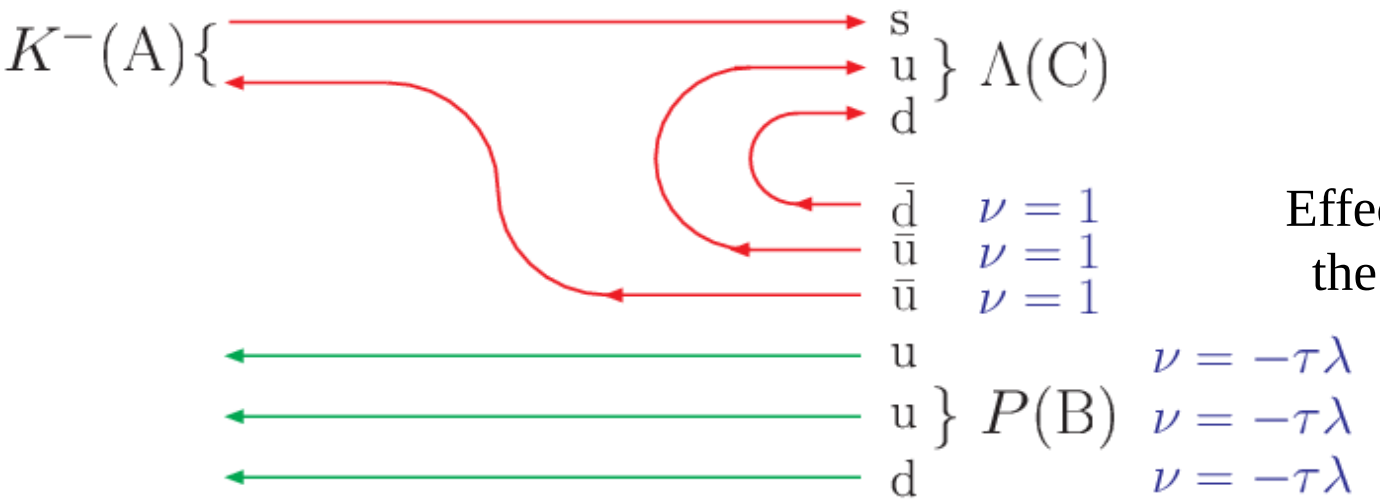

Fig. 9. Quark diagram for the reaction $K^- + p \rightarrow \Lambda + X$. $\nu_A=[3 - 3\tau\,\lambda] >0$.

Fig.9 shows that there are three spectator antiquarks in the reaction, which create a strong chromomagnetic field for the test s-quark, which transfers the spin of the Λ-hyperon. This field leads also to the precession of the spin of the s-quark and the corresponding oscillation of the polarization of the Λ-hyperon, since the value of the parameter $\nu_A=[3 - 3\tau\,\lambda] \approx 3$ is large. To calculate the value of ν_A, it is necessary to sum all quarks and antiquark-spectators with weights ν indicated to the right of them [1,2]. The oscillation frequency of the Λ-hyperon polarization is proportional to ν_A.
Similar quark diagrams exist for other hyperons and antihyperons, produced by meson beams. The value of $\nu_A=[3 - 3\tau\,\lambda] \approx 3$ in the fragmentation region of hadron A (meson) is the same for all meson beams. **$\lambda = -0.13529\pm0.00009$, $\tau = 0.02896\pm0.00009$ for 125 reactions.**

Calculations of the polarization of Λ-hyperons in meson beams

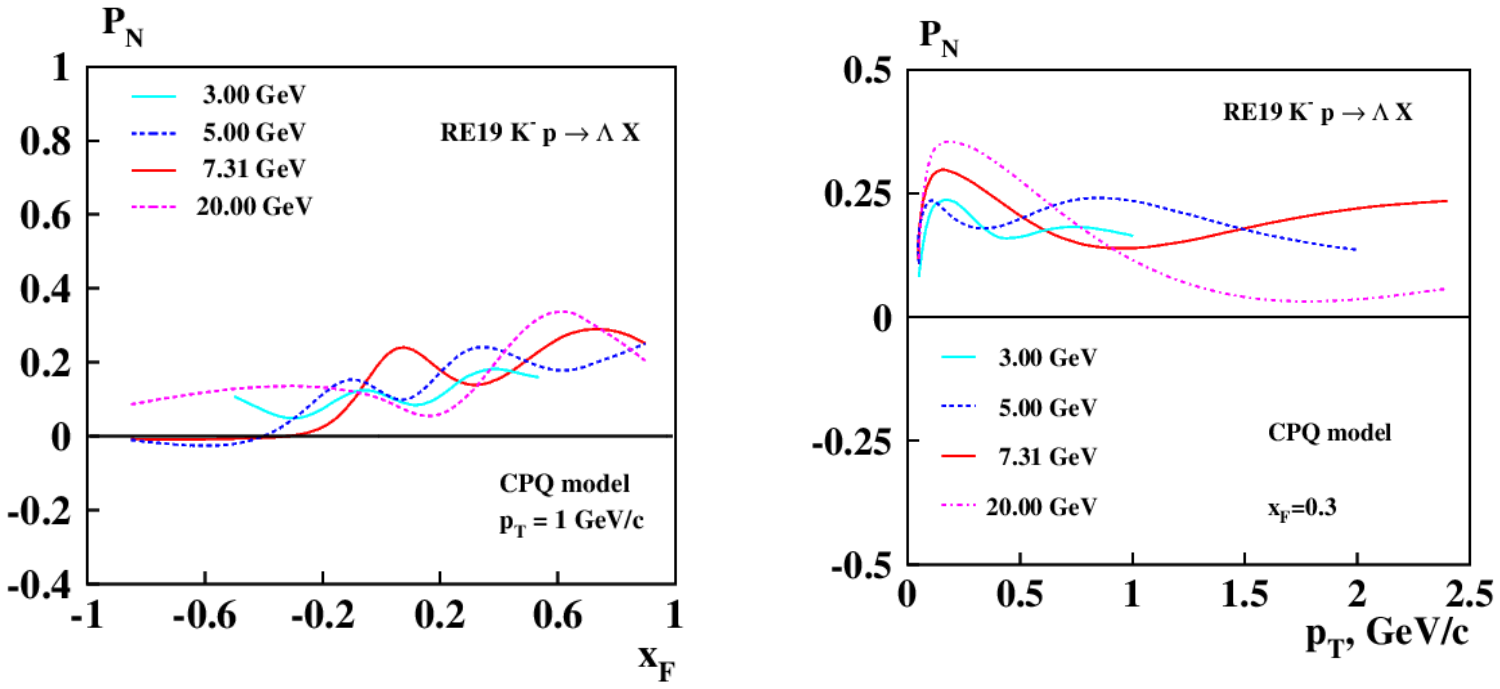

Fig. 10. Calculations of $P_N(x_F,p_T)$ according to the CPQ model for the reaction $K^- + p \rightarrow \Lambda + X$.

$P_N(x_F)$ tends to increase and oscillate as x_F increases. $P_N(p_T)$ increases rapidly as p_T approaching to 0.2 GeV/c.

A nonmonotonic energy dependence of $P_N(p_T)$ is predicted for $p_T > 0.2$ GeV/c, which is due to quark spin precession.

Calculations of the polarization of $\tilde{\Lambda}$-hyperons in K^+ meson beam

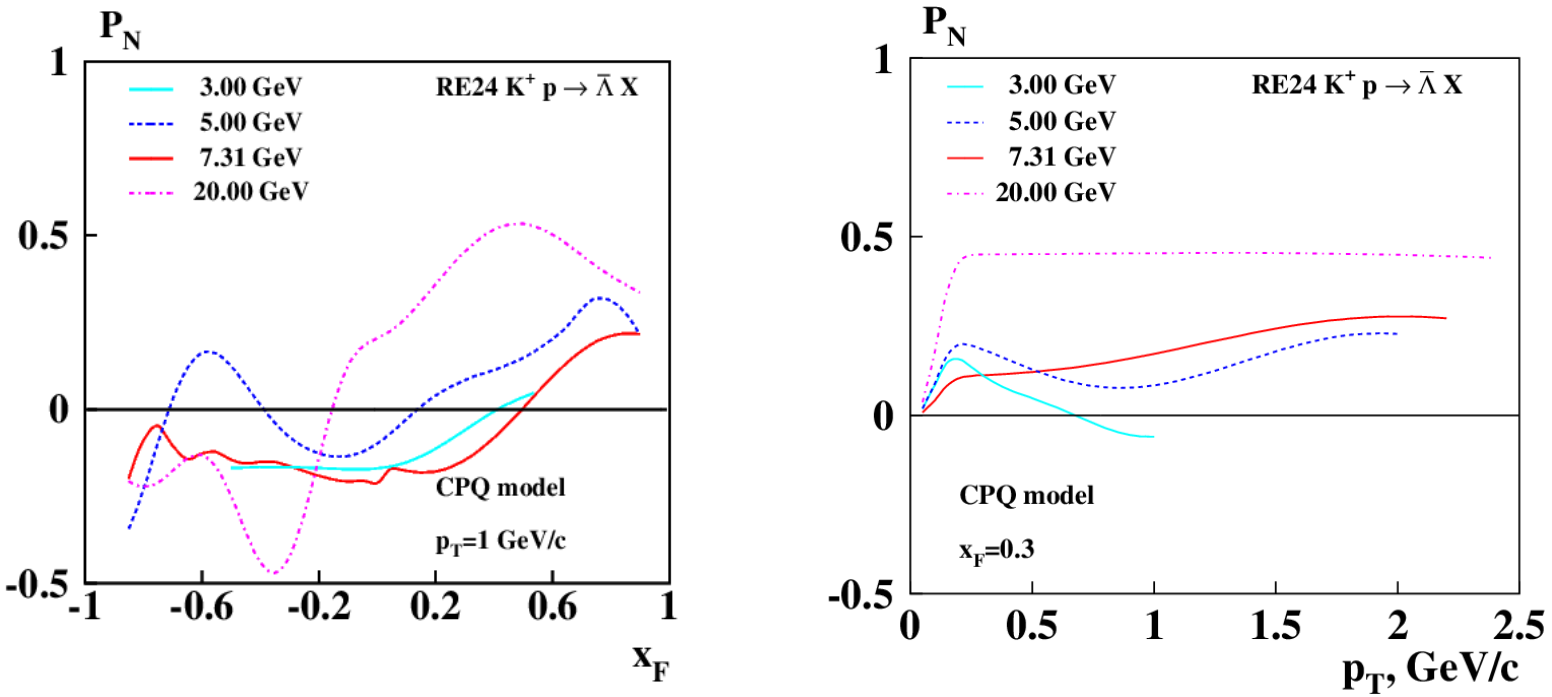

Fig. 11. Calculations of $P_N(x_F,p_T)$ according to the CPQ model for the reaction $K^+ + p \rightarrow \tilde{\Lambda} + X$.

A significant dependence of $P_N(x_F)$ on energy and x_F is predicted.

An increase in $P_N(p_T)$ is predicted with increasing $\sqrt{s}$ and p_T>0.7 GeV/c.

Calculations of the polarization of Λ-hyperons in K^+ meson beam

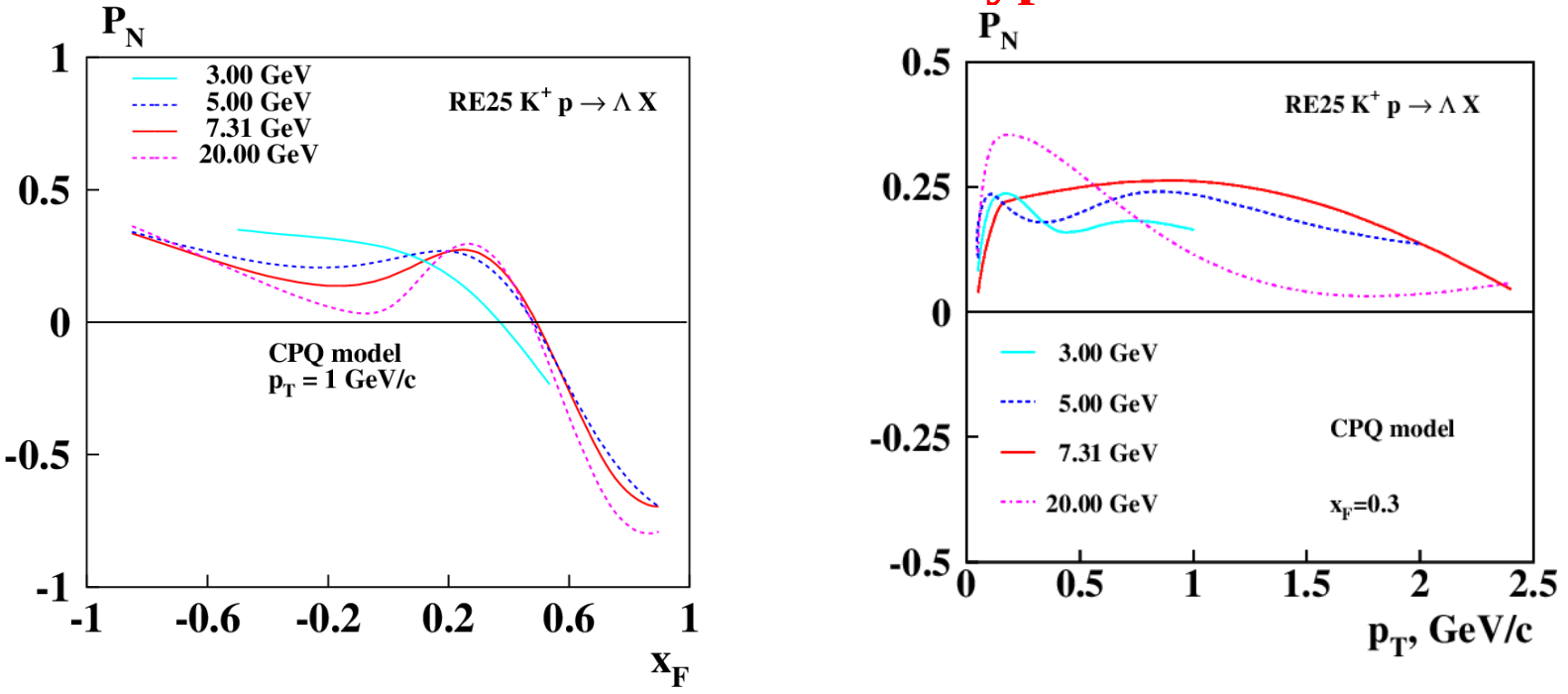

Fig. 12. Calculations of $P_N(x_F,p_T)$ according to the CPQ model for the reaction $K^+ + p \rightarrow \Lambda + X$.

A nonmonotonic dependence of $P_N(x_F)$ is expected with a change of sign at $x_F \approx 0.5$. Significant negative polarization is predicted at $x_F \approx 0.8$.

Significant energy dependence $\sqrt{s}$ is expected in the region $0.2 \leq p_T \leq 1.8$ GeV/c.

Calculations of the polarization of $\tilde{\Lambda}$-hyperons in K^- meson beam

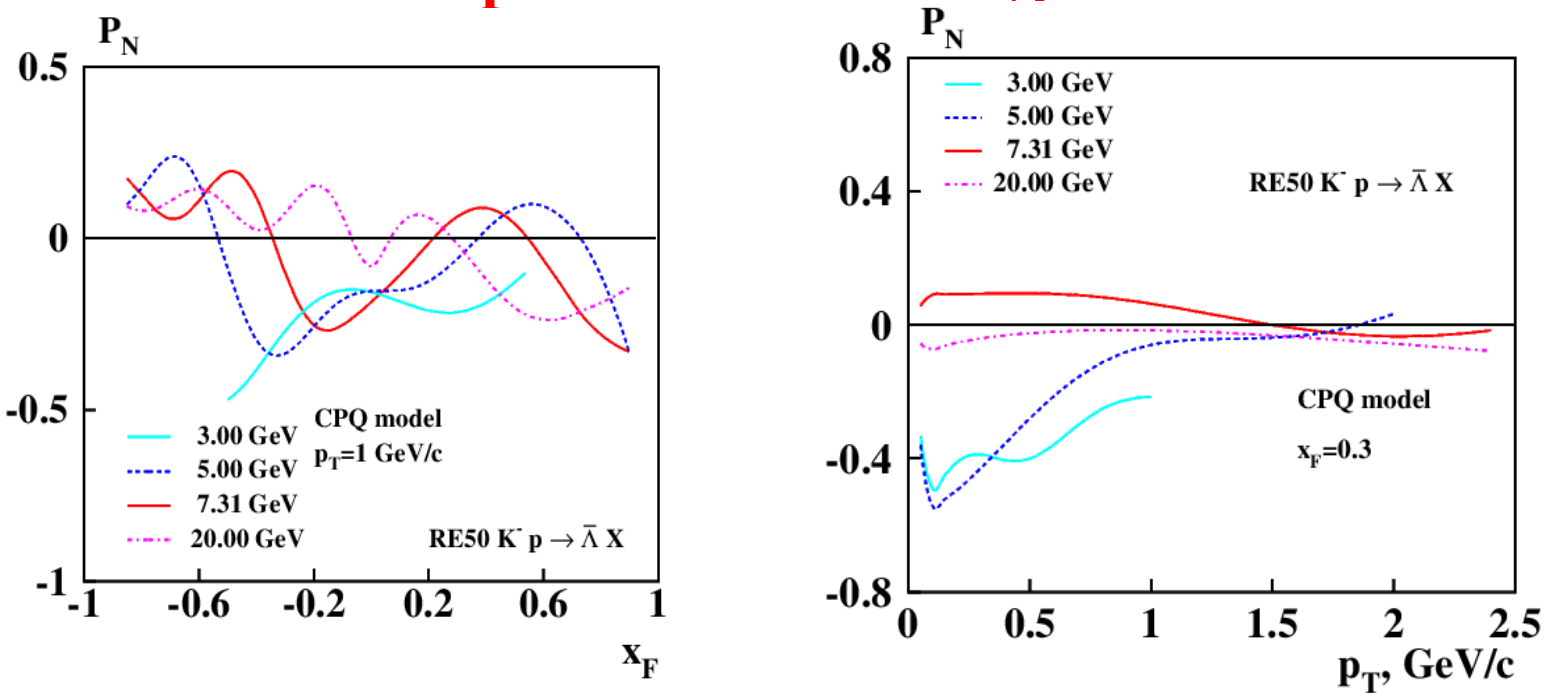

Fig. 13. Calculations of $P_N(x_F,p_T)$ according to the CPQ model for the reaction $K^- + p \rightarrow \tilde{\Lambda} + X$.

Oscillation of $P_N(x_F)$ is predicted.

A strong energy dependence in the region p_T=0.2-0.5 GeV/c and a large negative polarization are predicted for $\sqrt{s} \leq 6$ GeV.

Calculations of the polarization of Λ-hyperons in π^- meson beam

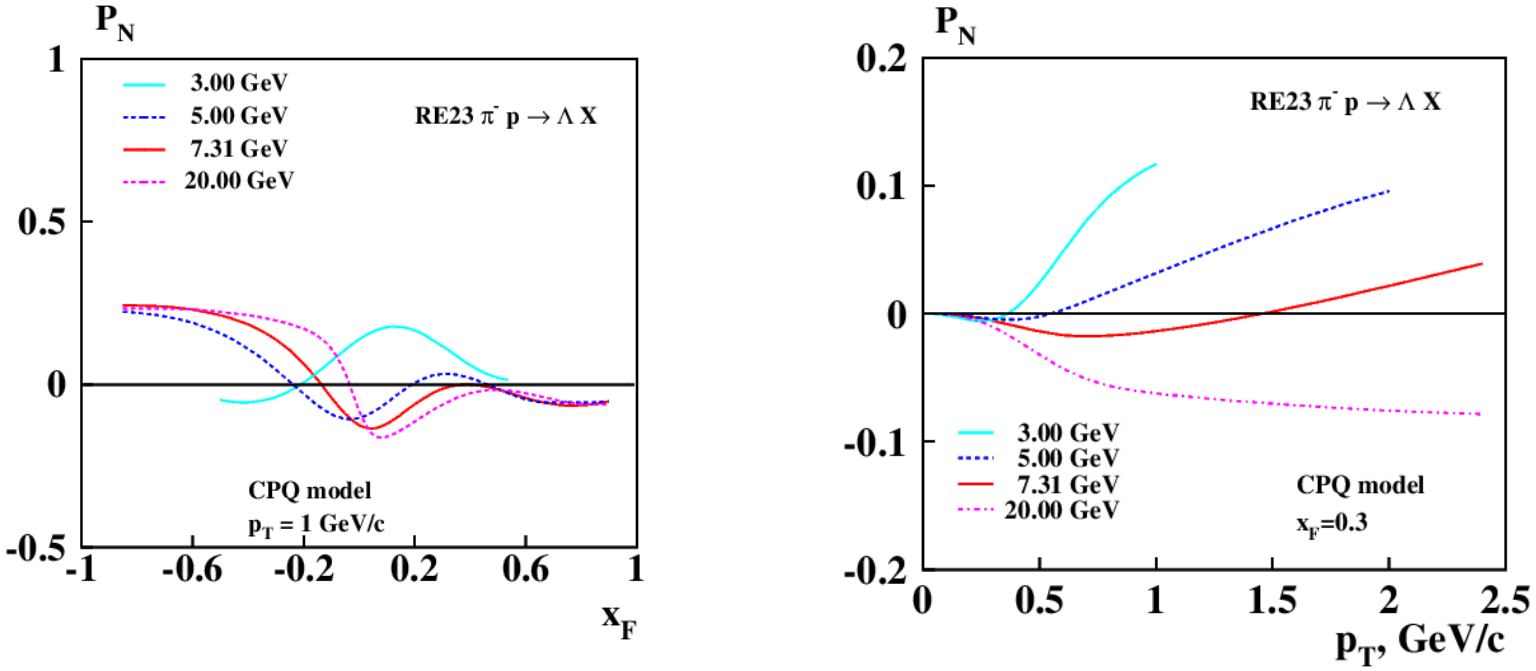

Fig. 14. Calculations of $P_N(x_F,p_T)$ according to the CPQ model for the reaction $\pi^- + p \rightarrow \Lambda + X$.

The most significant energy dependence of $P_N(x_F)$ is expected at $x_F = 0.05$, as well as in the range of negative x_F values.

An increase in $P_N(p_T)$ is predicted with a change in the polarization sign as the energy decreases.

Calculations of the polarization of Λ-hyperons in π^+ meson beam

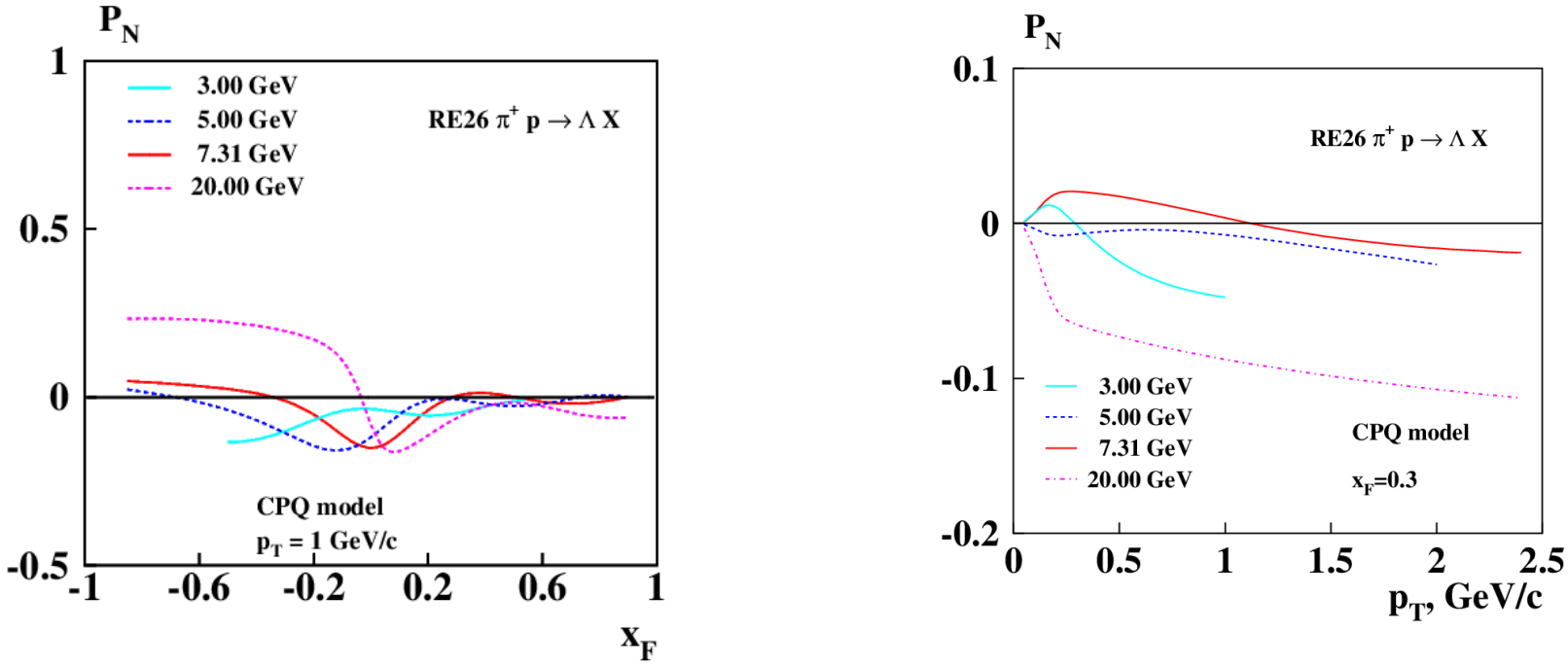

Fig. 15. Calculations of $P_N(x_F,p_T)$ according to the CPQ model for the reaction $\pi^+ + p \rightarrow \Lambda + X$.

Significant negative polarization is expected at energies of 3 and 20 GeV.
The dependence of $P_N(p_T)$ on $\sqrt{s}$ is nonmonotonic.

Near zero polarization is expected for large x_F>0.4, for $\pi^{\pm} + p \rightarrow \Lambda + X$ reactions.

Calculations of the polarization of $\tilde{\Lambda}$-hyperons in π^- meson beam

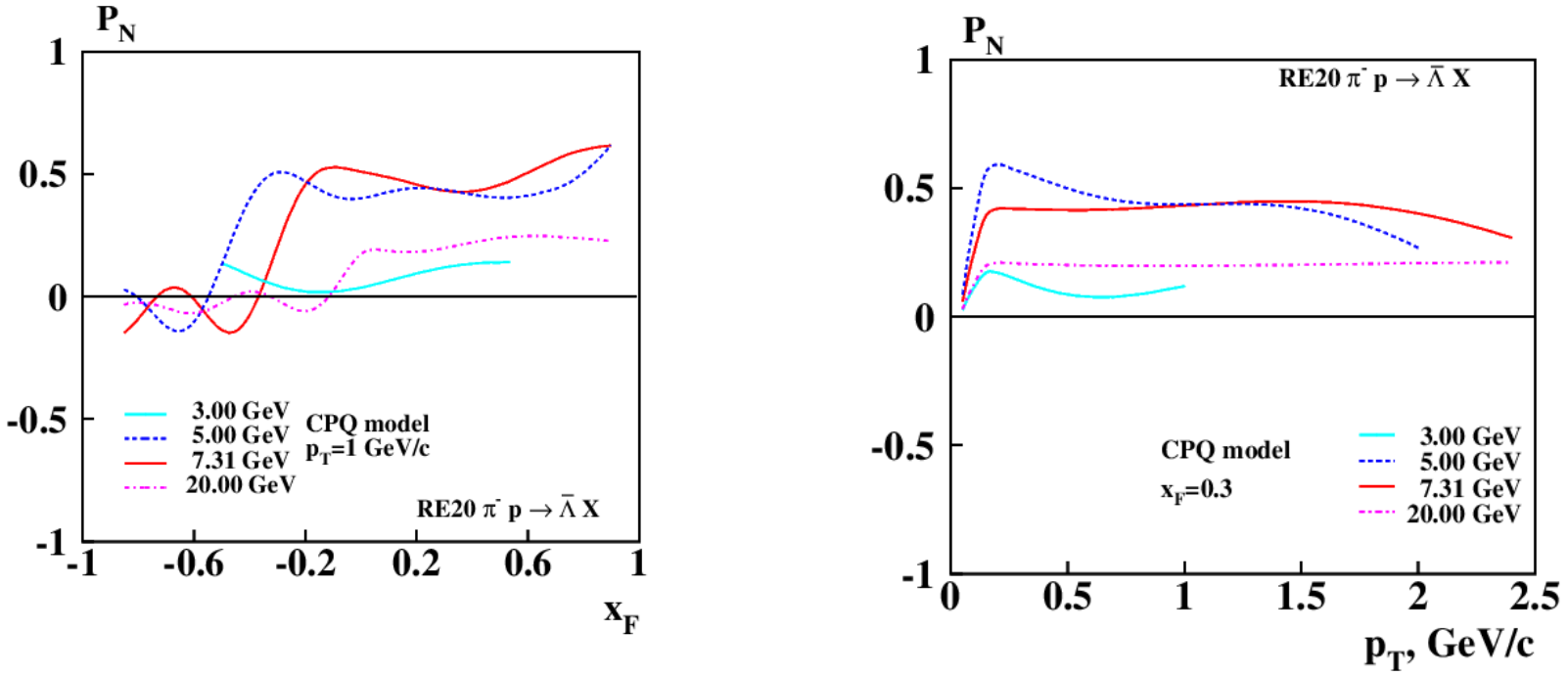

Fig. 16. Calculations of $P_N(x_F,p_T)$ according to the CPQ model for the reaction $\pi^- + p \rightarrow \tilde{\Lambda} + X$.

The $P_N(x_F)$ oscillates and varies over a wide range as $\sqrt{s}$ and x_F vary.

The dependence of $P_N(p_T)$ on $\sqrt{s}$ is nonmonotonic.

Large positive $P_N(x_F)$ is expected for $\sqrt{s} = 3 – 12$ GeV and $x_F > 0$.

Comparison of the polarization of Λ-hyperons in meson beams

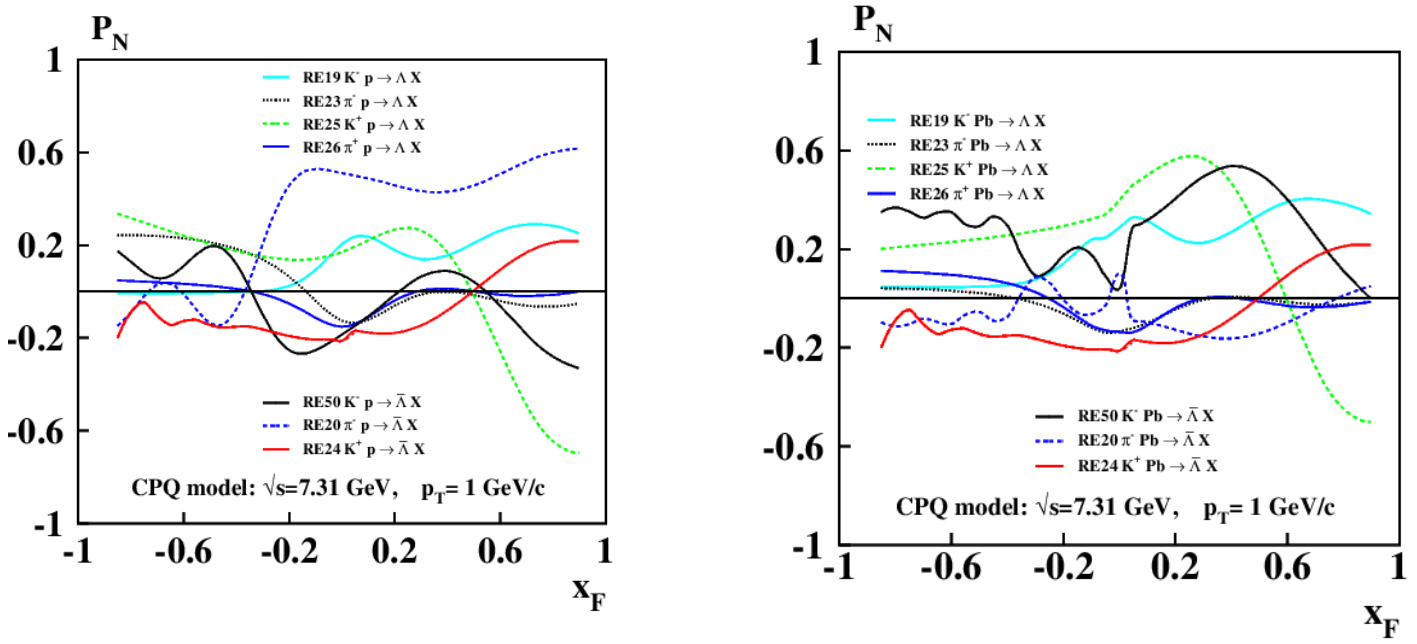

Fig. 17. Calculations of $P_N(x_F)$ according to the CPQ model for the reactions $K^{\pm}$ ($\pi^{\pm}$) + p(pB) → Λ($\tilde{\Lambda}$) + X at an energy of $\sqrt{s}$=7.31GeV and p_T=1 GeV/c.

Oscillation of $P_N(x_F)$, dependence on atomic weight is predicted. The most significant positive polarization is predicted for the reactions π^- + p(A) → Λ + X and π^- + p(A) → $\tilde{\Lambda}$ + X. Several reactions pass through zero at x_F = ±0.5 and -0.4.

A particularly strong A-dependence of polarization is expected for the reaction π^- + p(A) → $\tilde{\Lambda}$ + X.

Energy dependence of the polarization of $\tilde{\Lambda}$-hyperons in meson beams

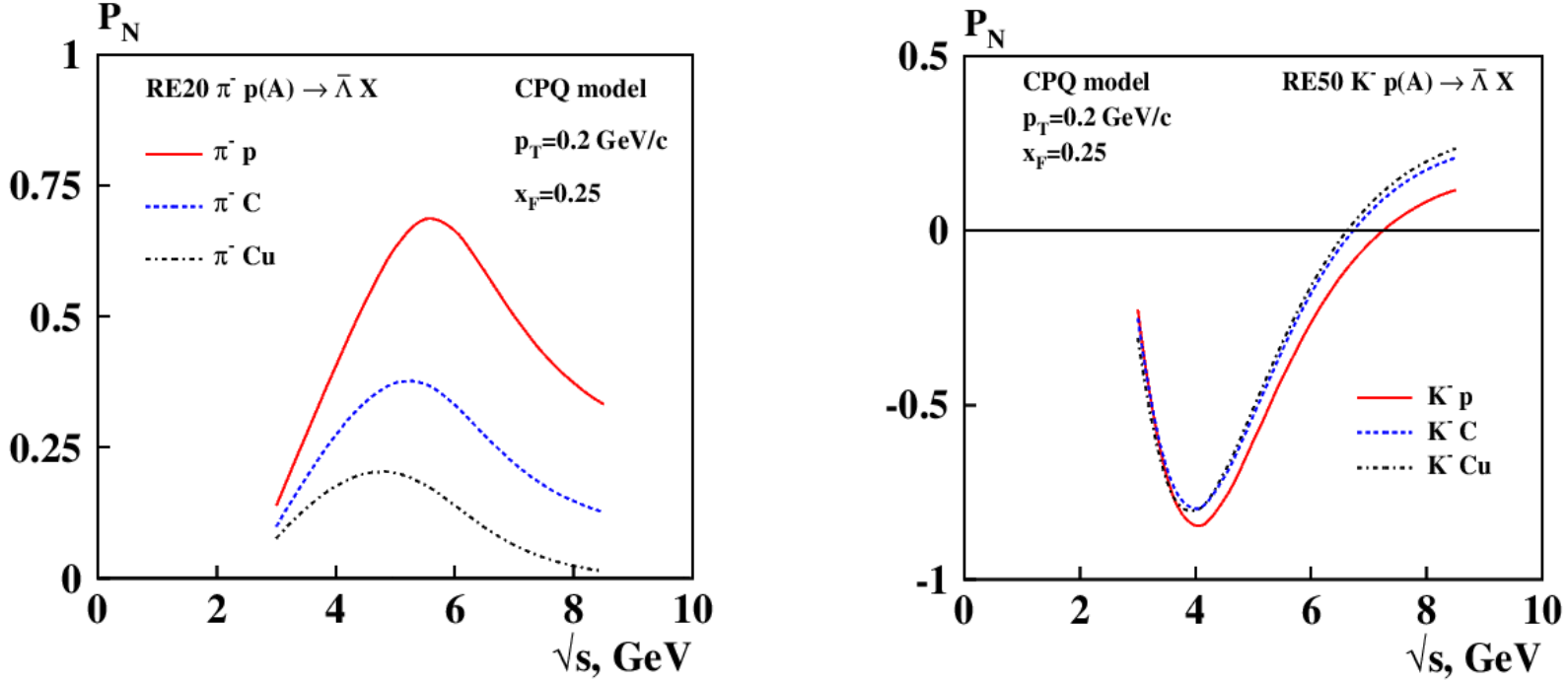

Fig. 18. Calculations of $P_N(\sqrt{s})$ according to the CPQ model for the reactions K^- $(\pi^-) + p(A) \rightarrow \tilde{\Lambda} + X$ at $x_F = 0.25$ and $p_T = 0.25$ GeV/c.

Resonance like behavior of $P_N(\sqrt{s})$, dependence on atomic weight are predicted for the reactions $\pi^- + p(A) \rightarrow \tilde{\Lambda} + X$ and $K^- + p(A) \rightarrow \tilde{\Lambda} + X$. The height of the polarization maximum decreases with increasing target atomic weight (A). The position of the polarization maximum shifts towards smaller values of $\sqrt{s}$ as A increases, from 5.5 GeV to 4.7 GeV for the reaction $\pi^- + p(A) \rightarrow \tilde{\Lambda} + X$. This is due to the dependence of the $\tilde{s}$-quark spin precession rate in a chromomagnetic field on $\sqrt{s}$ and the attraction between the active test $\tilde{s}$-quark and spectator quarks.

References

[1] V.V. Abramov, Phys. Atom. Nucl. **72** (2009) 1872.
[2] V.V. Abramov, A. Aleshko, V.A. Baskov, E. Boos, V. Bunichev et al., Phys.Part.Nucl. 52 (2021) 6, 1044-1119, e-Print: 2102.08477 [hep-ph], JINR preprint E2-2021-12.
[3] S.A Gourlay et al., Phys.Rev.Lett. 56(1986) 2244.
[4] M.Baubillier et al., Nucl.Phys. B148 (1979) 18.
[5] H.Grassler et al., Nucl.Phys. B136 (1978) 386.
[6] H.Abramowicz et al., Nucl.Phys.B105 (1976) 222.
[7] F.Barreiro et al., Phys. Rev. D17 (1978) 66.
[8] P.V.Chliapnikov et al., Nucl. Phys. B112 (1976) 1.
[9] M.L Faccini-Turluer et al., Z.Phys. C1(1979) 19.
[10] M. Barth et al, Z.Phys. C10 (1981) 205.
[11] B.Adeva et al., Z.Phys. C26 (1984) 359.
[12] R.Sugahara et al., Nucl.Phys. B156 (1979) 237.
[13] P.H.Stuntebeck et al., Phys.Rev.D9 (1974) 608.
[14] I.V.Azhinenko et al., Phys. Lett. 121B (1983) 183.
[15] W.Barletta et al., Nucl.Phys. B51 (1973) 499.
[16] S.Barlag et al., Phys.Lett. B325 (1994) 531.
[17] V.V. Abramov, JPS Conf.Proc. 37 (2022) 020901.

[19] M.G.Ryskin, *Sov.J.Nucl.Phys.* 48 (1988) 708-712, *Yad.Fiz.* 48 (1988) 1114-1121.
[20] A.B.Migdal, S.B.Khokhlachev, The structure of a gluon string, *JETP Lett.* 41 (1985) 194-198, *Pisma Zh.Eksp.Teor.Fiz.* 41 (1985) 159-162.

Conclusions and outlook

Calculations of the polarization of Λ-hyperons and antihyperons in meson beams are carried out.

Dependence of $P_N(x_F, p_T, \sqrt{s}, A)$ on kinematical variables, reaction type and the atomic weight of the target is predicted.

For the most of reactions, oscillations of $P_N(x_F)$ are expected due to the precession of the spin of s-quarks and a significant value of the parameter $\nu_A \approx 3$ (strong field case). The effect of the resonance like dependence of $P_N(\sqrt{s})$ in the production of $\tilde{\Lambda}$ in π^- and K^- beams is expected.

The results of hyperon polarization calculations can be verified at the U-70 accelerator at the NRC “Kurchatov Institute" - IHEP (at the SPASCHARM facility).

This work was supported by a grant № 22-12-00164 from the Russian Science Foundation.

Thank you for attention!

BACKUP SLIDES

The role of color factor λ

When taking into account the interaction of a test quark with the field created by a moving spectator quark, it is necessary to take into account the color factor for the corresponding pair of quarks (spectator and test quarks). An analysis of the data have shown that the quark-antiquark pair interacts predominantly in the color-singlet state with the color factor $\mathbf{C_F = 4/3}$, and the quark-quark or antiquark-antiquark pair interacts in the color-antitriplet state with $\mathbf{C_F = 2/3}$. For a hydrogen-like potential, the wave function of two quarks or a quark and an antiquark at zero coordinate is proportional to $\mathbf{|\Psi(0)| \sim (C_F \alpha_S)^{3/2}}$ [3], which leads to the ratio of contributions from qq and $q\tilde{q}$ interactions to ν_A of the order

$$\mathbf{\lambda \approx -|\Psi qq(0)|^2/|\Psi q\tilde{q}(0)|^2 = -1/8.} \qquad (1)$$

The minus sign in (1) takes into account the opposite sign of the field created by a moving spectator quark and a moving spectator antiquark. Experimentally, the value of the global parameter **λ**, obtained as a result of the global fit of the polarization data, turned out to be $\mathbf{\lambda = -0.1363 \pm 0.0003}$. A value, more close to the experimental one is given by the formula $\lambda = 1 - \exp(1/8) \approx -0.1331$, which can be considered as a generalization of formula (1).

[15] Baranov S.P. On the production of doubly flavored baryons in p p, e p and gamma gamma collisions // Phys. Rev. — 1996. — V. D54 — P. 3228–3236.

Effective number of nucleons in the target (A_{eff}) in the case of hA collisions

The effective number of nucleons in the target nucleus is equal to their number in a tube of radius $R_b = r_0 A_b^{1/3}$:

$$A_{eff} = A_2\{1 - [1 - (A_b/A_2)^{2/3}]^{3/2}\} \approx 0.69 A_2^{1/3}. \qquad (4)$$

If $A_2 < A_b$, then $A_{eff} = A_2$. For nucleon target, $A_{eff} = 1$.

A_b is the free model parameter obtained from the global fit of 87 inclusive single-spin reactions.

Fit: $A_b = 0.314 \pm 0.006$; $R_b = r_0 A_b^{1/3} \approx 0.82 \pm 0.02$ fm, (5)

where A_2 – target nucleus atomic weight, $r_0 = 1.2$ fm.

For an incident hadron or lepton, we set $A_1 = 1$.

Equations for A_N, P_N and $(\rho_{00}-1/3)$

$$P_N \approx C(\sqrt{s})\, F(p_T, A)[G(\varphi_A) - \sigma G(\varphi_B)], \quad (3)$$

$$G(\varphi_A) = [1 - \cos\varphi_A]/\varphi_A + \varepsilon\varphi_A, \quad \text{spin precession and S-G force,} \quad (4)$$

where $\varepsilon = -0.00497 \pm 0.00009$ - global, σ – local parameter.

$$C(\sqrt{s}) = v_0/[(1 - E_R/\sqrt{s})^2 + \delta_R^2]^{1/2}, \quad \text{spin precession vs } E_Q \quad (5)$$

$$F(p_T,A) = \{1 - \exp[-(p_T/p^0_T)^{2.5}]\}(1 - \alpha_A \ln A), \quad \text{color form factor} \quad (6)$$

$$v_0 = -D_r\, g^a_Q\, P_Q /2(g^a_Q - 2), \quad \text{sign and magnitude of } A_N \text{ and } P_N \quad (7)$$

$$\varphi_A = \omega^0_A y_A, \quad \varphi_B = \omega^0_B y_B, \quad \text{integral "precession angles"} \quad (8)$$

$$y_A = x_A - (E_0/\sqrt{s} + f_0)[1 + \cos\theta_{cm}] + a_0[1 - \cos\theta_{cm}], \quad (9)$$

$$y_B = x_B - (E_0/\sqrt{s} + f_0)[1 - \cos\theta_{cm}] + a_0[1 + \cos\theta_{cm}], \quad (10)$$

$$x_A = (x_R + x_F)/2, \quad x_B = (x_R - x_F)/2. \quad \text{scaling variables} \quad (11)$$

$$\omega^0_{A(B)} = g_s \alpha_s \nu_{A(B)}\, m_r(g^a_Q - 2)/M_Q, \quad m_r = 0.2942 \pm 0.0072 \text{ GeV}. \quad (12)$$

$\nu_{A(B)}$ - effective contributions of the spectator quarks to the field B^a.

Oscillation of A_N and P_N in a strong color field

$$P_N \approx C(\sqrt{s})\, F(p_T, A)[G(\varphi_A) - \sigma G(\varphi_B)], \quad (3)$$

$$G(\varphi_A) = [1 - \cos\varphi_A]/\varphi_A + \varepsilon\varphi_A, \quad (4)$$

is a result of the spin precession and S-G force

were φ_A, φ_B – are the integral "spin precession angles" in the fragmentation regions of the projectile A and the target B, respectively. ε = -0.00497 ± 0.00009.
Analysis shows that effective length S of the field B^a is: $S_0 x_A$ or $S_0 x_B$ for fragmentation regions of colliding particles A and B, where S_0 is about 1 fm.

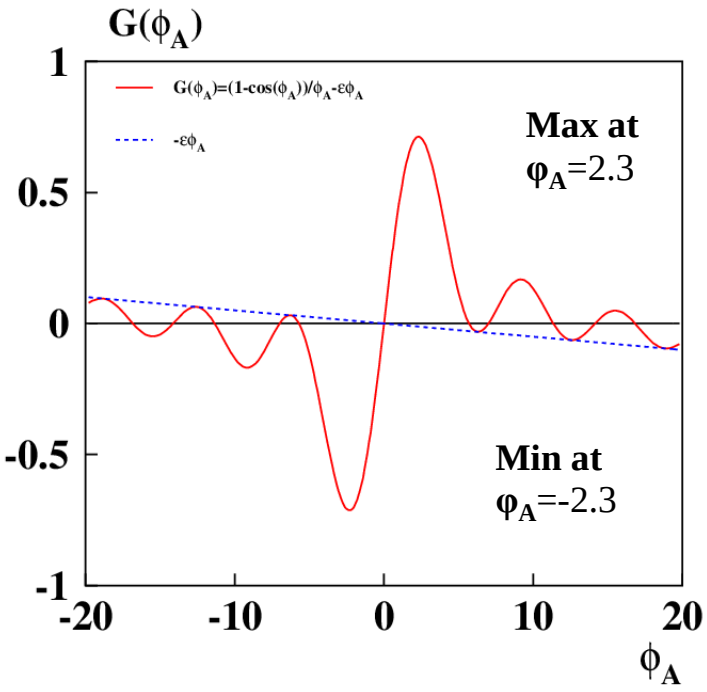

$$\varphi_A = \omega^0{}_A y_A, \quad \varphi_B = \omega^0{}_B y_B; \quad (8)$$

$$\omega^0{}_{A(B)} = g_s \alpha_s \nu_{A(B)}\, m_r (g^a{}_Q - 2)/M_Q, \quad (12)$$

$$m_r = 0.2942 \pm 0.0072\ \text{GeV}; \quad \alpha_s = g_s{}^2/4\pi;$$

$$y_A = x_A - (E_0/\sqrt{s} + f_0)[1 + \cos\theta_{cm}] + a_0[1 - \cos\theta_{cm}] \quad (9)$$

$$y_B = x_B - (E_0/\sqrt{s} + f_0)[1 - \cos\theta_{cm}] + a_0[1 + \cos\theta_{cm}] \quad (10)$$

$x_A = (x_R + x_F)/2$, $x_B = (x_R - x_F)/2$ - scaling variables. (11)

$\nu_{A(B)}$ - effective contributions of the spectator quarks to the field B^a.

Quark counting rules for ν_A (A + B → C + X)

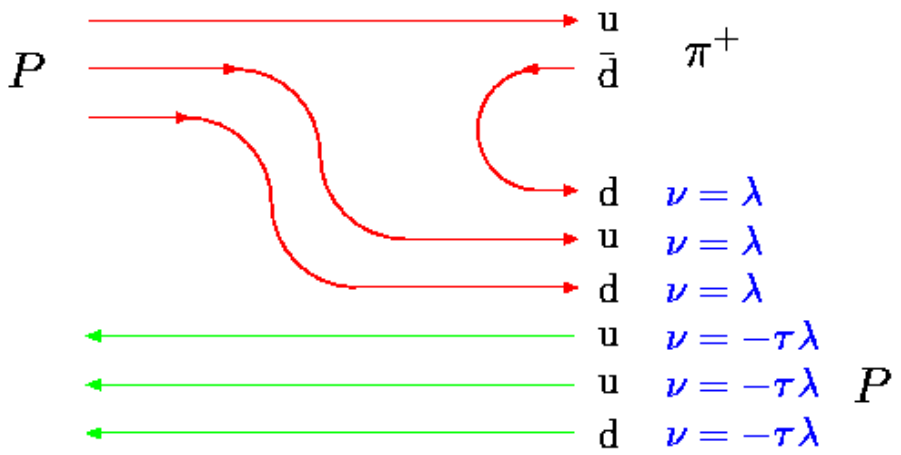

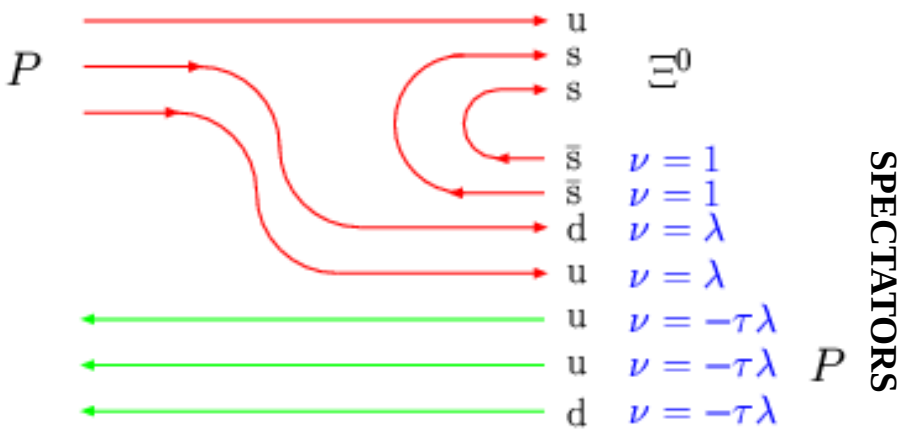

$\int \mathbf{E^a} \sim \int \mathbf{B^a} \sim \nu_A = [3\lambda - 3\tau\lambda] < 0$; $\int \mathbf{E^a} \sim \int \mathbf{B^a} \sim \nu_A = [2 + 2\lambda - 3\tau\lambda] > 0$

$\mathbf{A_N \sim P_U \nu_A (g^a_U - 2)/2M_U > 0;}$ $\mathbf{P_N \sim \nu_A (g^a_S - 2)/2M_S < 0.}$

qq, q̃q̃ -SU(3)$_c$ antitriplet, weight $\nu = \lambda$; $C_F = 2/3$ – color factor

qq̃, q̃q -SU(3)$_c$ singlet, weight $\nu = 1$. $C_F = 4/3$ – color factor

- S.P. Baranov, Phys. Rev. D54, 3228 (1996). $|\psi|^2 \sim (C_F \alpha_S)^3$. (16)
- $\lambda = -|\psi_{qq}(0)|^2 / |\psi_{q\,\tilde{q}}(0)|^2 \approx 1 - e^{1/8} \approx -0.1332$ **color factor** (17)
- $\lambda = -0.1363 \pm 0.0003$, $\tau = 0.0267 \pm 0.0012$, **fit for 85 reactions.**

Quark counting rules for $p\uparrow + p \rightarrow \pi^+ + X$

$\nu_A = 3\lambda - 3\tau\lambda = -0.398$ (3)

$\nu_B = \nu_A$, where global parameters for 85 (3608 points) reactions are:

$\lambda = -0.1363 \pm 0.0003$, (4)

$\tau = 0.0267 \pm 0.0005$. (5)

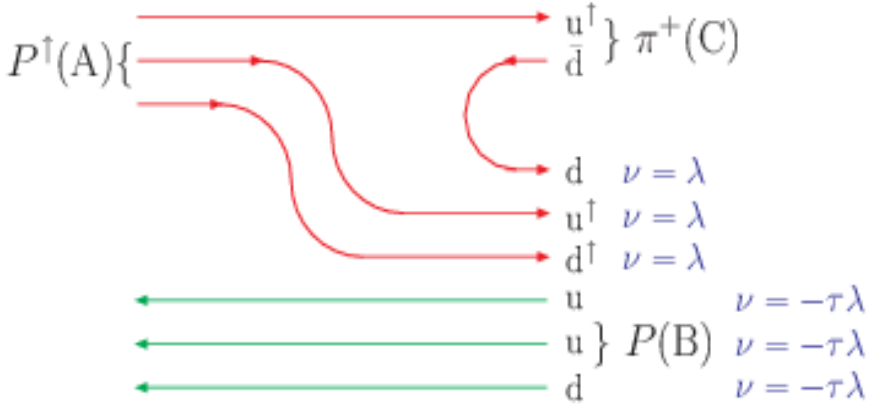

SPECTATORS

For comparison is shown a quark flow in reaction $p\uparrow + p \rightarrow p + X$.

The effective number of quarks is:

$\nu_A = 2 + 2\lambda - 3\tau\lambda = 1.738$, (6)

$\nu_B = \nu_A$.

So, in case of reaction $p\uparrow + p \rightarrow p + X$ ν_A is approximately 4 times higher, than in case of $p + p \rightarrow \pi^+ + X$. As a result, $A_N(x_F)$ should oscillates with approximately 4 times higher frequency for $p\uparrow + p \rightarrow p + X$ reaction. The sign $\mathbf{(-g_S \nu_A P_Q)}$ of A_N for proton must be opposite (negative) at small x_F.

and $p\uparrow + p \rightarrow p + X$

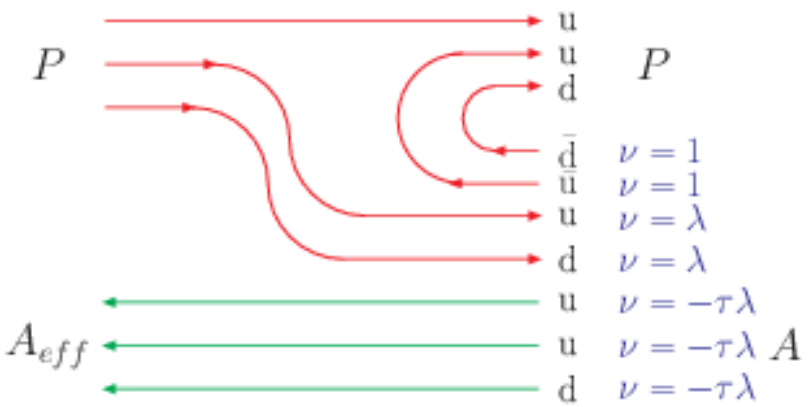

SPECTATORS

Quark flow diagrams for the cascade antihyperon production

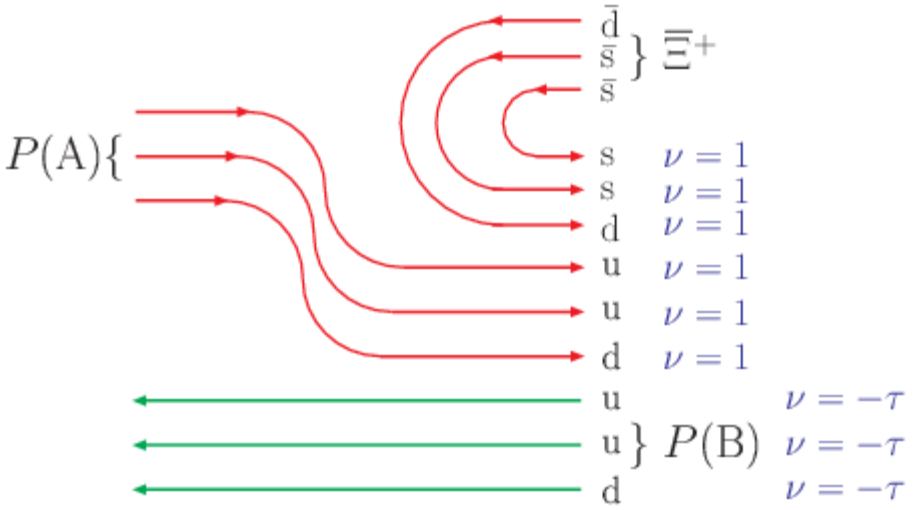

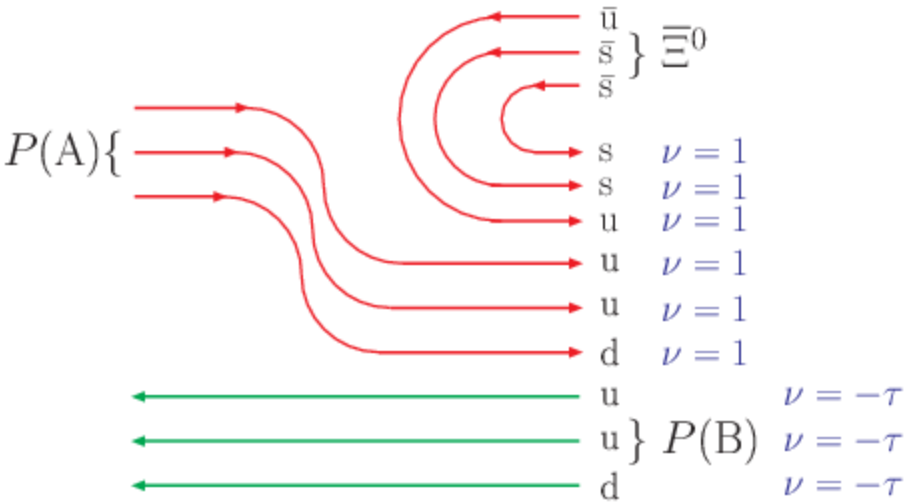

In case of $\bar{\Xi}^+$ and $\bar{\Xi}^0$ production in pA-collisions the quark flow diagrams look similar. But constituent masses of u and d are different.

Six spectator quarks interact with each of active valence test quark of antihyperon and create a very strong chomomagnetic field.

Large values of $\nu_A = \nu_B = 6 - 3\tau$ leads to a very high quark spin precession frequency and the corresponding high oscillation frequency $\boldsymbol{\omega^0_{A(B)}}$ for $P_N(x_F)$, which is proportional to ν_A or ν_B.

Quark counting rules for the p + p → Ξ⁻ + X

$\nu_A = (2 + 2\lambda) - 3\tau\lambda = 1.738$ (3)

$\nu_B = \nu_A$, where global parameters for 85 reactions are:

$\lambda = -0.1363 \pm 0.0003$,

$\tau = 0.0267 \pm 0.0005$.

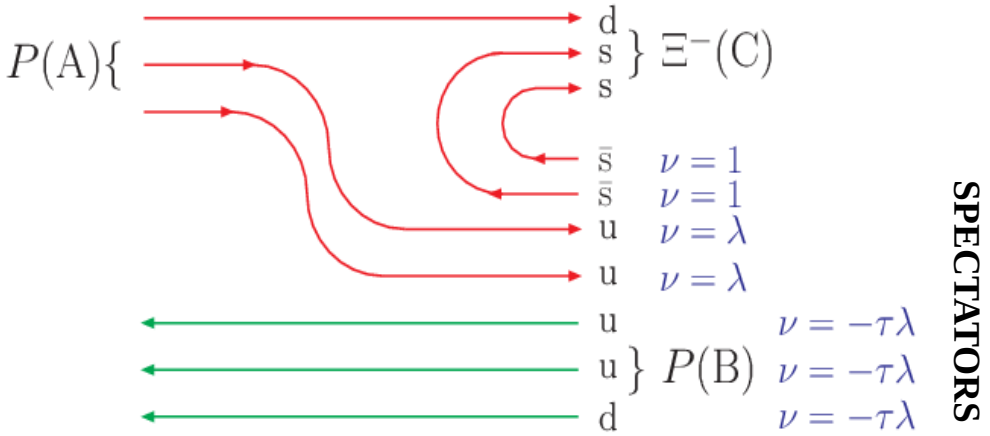

For comparison is shown a quark flow in reaction p + p → Λ + X.

The effective number of quarks is:

$\nu_A = (1 + \lambda) - 3\tau\lambda = 0.8746$ (4)

$\nu_B = \nu_A$.

So, in case of reaction p + p → Ξ⁻ + X ν_A is approximately two times higher, than in case of p + p → Λ + X.

As a result, $P_N(x_F)$ should oscillates with approximately two times higher frequency for p + p → Ξ⁻ + X reaction.

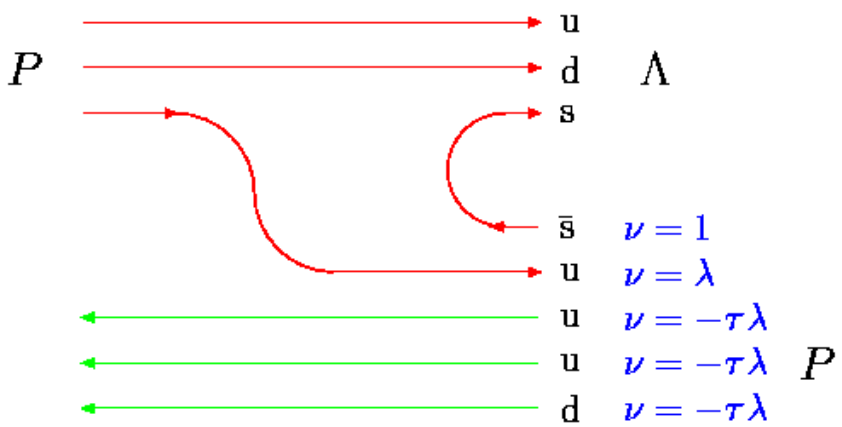

pp → Λ + X production quark diagram.

Color flux tube counting.

Model parameters (global and local)

1) $m_s = 98\pm2$ MeV; 2) $m_c = 1264\pm17$ MeV; 3) $\Delta\mu^a_u = -0.4839\pm0.0017$;

4) $\Delta M_u = 0.2665\pm0.0012$; 5) $\Delta M_d = 0.3033\pm0.0013$; 6) $\Delta M_s = 0.3703\pm0.0020$;

7) $\tau = 0.0267\pm0.0005$; 8) $\lambda = -0.1363\pm0.0003$; 9) $\varepsilon = -0.00497\pm0.00009$;

10) $W_0 = 275.6\pm1.3$ GeV; 11) $P_N = 84.7\pm0.4$ GeV; 12) $m_r = 0.3573\pm0.0016$ GeV;

13) $n_q = 4.671\pm0.018$; 14) $A_a = 10.35\pm0.55$; 15) $A_b = 0.3084\pm0.0012$;

16) $A_T = 59.6\pm5.8$; 17) $\delta_R = 0.2907\pm0.0026$; 18) $a_f = 3.092\pm0.047$;

19) $V_T = 0.1437\pm0.062$; 20) $p_m = 0.152\pm0.038$ GeV; 21) $a_{81} = 1.622\pm0.050$;

22) $a_{56} = 0.4220\pm0.0013$ GeV; 23) $E_0 = -83.8\pm0.4$ GeV; 23) $a_{51} = 0.0236\pm0.0015$;

25) $E_c = 0.000511\pm0.000003$; 26) $a_{41} = 0.1428\pm0.0013$; 27) $\eta = -1.761\pm1.18$;

$W_0 \approx m_p^2/m_q \approx 255\pm24$ GeV; $m_q \approx (m_u+m_d)/2 \approx 3.45\pm0.33$MeV; $\lambda \approx 1-\exp(1/8) \approx -0.133$;

Global Data Analysis: A_N

Inclusive reactions, in which was measured single-spin asymmetry in hadron-hadron collisions (26 reactions).

№	Reaction	№	Reaction	№	Reaction
1	$p^{\uparrow}\, p(A) \rightarrow \pi^{+}$	10	$p^{\uparrow}\, A \rightarrow J/\psi^{\uparrow}$	19	$\pi^{+}\, p^{\uparrow} \rightarrow \pi^{+}$
2	$p^{\uparrow}\, p(A) \rightarrow \pi^{-}$	11	$p^{\uparrow}\, p \rightarrow \eta$	20	$\pi^{-}\, p^{\uparrow} \rightarrow \pi^{-}$
3	$p^{\uparrow}\, p \rightarrow \pi^{0}$	12	$d^{\uparrow}\, A \rightarrow \pi^{+}$	21	$\pi^{-}\, p^{\uparrow} \rightarrow \pi^{0}$
4	$p^{\uparrow}\, p(A) \rightarrow K^{+}$	13	$d^{\uparrow}\, A \rightarrow \pi^{-}$	22	$\pi^{-}\, d^{\uparrow} \rightarrow \pi^{0}$
5	$p^{\uparrow}\, p(A) \rightarrow K^{-}$	14	$\tilde{p}^{\uparrow}\, p \rightarrow \pi^{+}$	23	$K^{-}\, d^{\uparrow} \rightarrow \pi^{0}$
6	$p^{\uparrow}\, p \rightarrow K^{0}_{S}$	15	$\tilde{p}^{\uparrow}\, p \rightarrow \pi^{-}$	24	$K^{-}\, p^{\uparrow} \rightarrow \pi^{0}$
7	$p^{\uparrow}\, p(A) \rightarrow n$	16	$\tilde{p}^{\uparrow}\, p \rightarrow \pi^{0}$	25	$\pi^{-}\, p^{\uparrow} \rightarrow \eta$
8	$p^{\uparrow}\, p(A) \rightarrow p$	17	$\tilde{p}^{\uparrow}\, p \rightarrow \eta$	26	$\tilde{p}\, p^{\uparrow} \rightarrow \pi^{0}$
9	$p^{\uparrow}\, A \rightarrow \tilde{p}$	18	$\tilde{p}\, d^{\uparrow} \rightarrow \pi^{0}$		

Global Data Analysis: P_N

Inclusive reactions, in which was measured hyperon polarization in hadron-hadron collisions (31 reactions).

№	Reaction	№	Reaction	№	Reaction
27	$p\,p(A) \to \Lambda^{\uparrow}$	37	$\Sigma^{-}\,A \to \Sigma^{+\uparrow}$	48	$K^{-}\,p \to \Lambda^{\uparrow}$
28	$p\,A \to \Xi^{-\uparrow}$	38	$\Sigma^{-}\,A \to \Xi^{-\uparrow}$	49	$K^{-}\,A \to \Xi^{-\uparrow}$
29	$p\,A \to \Xi^{0\uparrow}$	39	$p\,A \to \tilde{\Lambda}^{\uparrow}$	50	$\pi^{-}\,A \to \Xi^{-\uparrow}$
30	$p\,A \to \Sigma^{+\uparrow}$	40	$\Sigma^{-}\,A \to \tilde{\Lambda}^{\uparrow}$	51	$\pi^{+}\,p \to \Lambda^{\uparrow}$
31	$p\,p \to p^{\uparrow}$	41	$p\,A \to \tilde{\Xi}^{+\uparrow}$	52	$K^{+}\,p \to \Lambda^{\uparrow}$
32	$p\,A \to \Sigma^{-\uparrow}$	42	$p\,A \to \tilde{\Xi}^{0\uparrow}$	53	$\pi^{-}\,p \to \Lambda^{\uparrow}$
33	$p\,A \to \Omega^{-\uparrow}$	43	$p\,A \to \tilde{\Sigma}^{-\uparrow}$	54	$K^{+}\,p \to \tilde{\Lambda}^{\uparrow}$
34	$\Sigma^{-}\,A \to \Lambda^{\uparrow}$	44	$\tilde{p}\,A \to \tilde{\Lambda}^{\uparrow}$	55	$\pi^{-}\,p \to \tilde{\Lambda}^{\uparrow}$
35	$p\,A \to \Sigma^{0\uparrow}$	45	$A_1+A_2 \to \Lambda^{\uparrow}$	56	$K^{-}\,p \to \tilde{\Lambda}^{\uparrow}$
36	$\Lambda\,A \to \Omega^{-\uparrow}$	46	$Au+Au \to \Lambda^{\uparrow(Glob)}$	57	$\pi^{-}\,A \to \tilde{\Xi}^{+\uparrow}$
		47	$Au+Au \to \tilde{\Lambda}^{\uparrow(GloB)}$		

Global Data Analysis: A_N, P_N, ρ_{00}

Other inclusive reactions, in which was measured vector meson polarization and lepton induced reactions (24 reactions).

№	Reaction	№	Reaction	№	Reaction
58	$p\,A \to J/\psi^{\uparrow}$	67	$n\,A \to K^*(892)^{-\uparrow}$	73	$e^+\,A \to \Lambda^{\uparrow}$
59	$\tilde{p}\,A \to J/\psi^{\uparrow}$	68	$n\,A \to K^*(892)^{+\uparrow}$	74	$e^+\,A \to \tilde{\Lambda}^{\uparrow}$
60	$p\,A \to Y(1S)^{\uparrow}$	69	$p\,p \to \varphi(1020)^{\uparrow}$	75	$e^+\,p^{\uparrow} \to \pi^+$
61	$p\,A \to Y(2S)^{\uparrow}$	70	$\tilde{p}\,p \to \rho(770)^{\uparrow}$	76	$e^+\,p^{\uparrow} \to \pi^-$
62	$p\,p \to Y(1S)^{\uparrow(\tilde{\lambda})}$	71	$AuAu \to \tilde{K}^*(892)^{0\uparrow}$	77	$e^+\,p^{\uparrow} \to K^+$
63	$p\,p \to Y(2S)^{\uparrow(\tilde{\lambda})}$	72	$AuAu \to \varphi(1020)^{\uparrow}$	78	$e^+\,p^{\uparrow} \to K^-$
64	$p\,p \to Y(3S)^{\uparrow(\tilde{\lambda})}$			79	$\mu^-\,6LiD^{\uparrow} \to h^+$
65	$\tilde{p}\,p \to Y(1S)^{\uparrow}$			80	$\mu^-\,6LiD^{\uparrow} \to h^-$
66	$\tilde{p}\,p \to Y(2S)^{\uparrow}$			81	$\nu_\mu\,A \to \Lambda^{\uparrow}$